Kinetics and Mechanism of Long-Chain Fatty Acid Transport into Phosphatidylcholine Vesicles from Various Donor Systems†

Richard M. Thomas,‡ Antonio Baici,§ Moritz Werder,‡ Georg Schulthess,|| and Helmut Hauser*,‡

Institute of Biochemistry, Swiss Federal Institute of Technology, ETH Center, Universitätstrasse 16, CH-8092 Zürich, Switzerland, Centre of Experimental Rheumatology, University of Zürich, Winterthurerstrasse 190, CH-8057 Zürich, Switzerland, and Department of Internal Medicine, Medical Policlinic, University Hospital, CH-8091 Zürich, Switzerland

Received July 24, 2001; Revised Manuscript Received October 17, 2001

ABSTRACT: The kinetics of long-chain fatty acid (FA) transfer from three different donor systems to unilamellar egg phosphatidylcholine (EPC) vesicles containing the pH-sensitive fluorophore pyranine in the vesicle cavity were determined. The transfer of long-chain FA from three FA donors, FA vesicles, unilamellar EPC vesicles containing FA, and bovine serum albumin−FA complexes to pyranine-containing EPC vesicles is a true first-order process, indicating that the FA transfer proceeds through the aqueous phase and not through collisional contacts between the donor and acceptor. A collisional mechanism would be at least bimolecular, giving rise to second-order kinetics. Evidence from stopped-flow fluorescence spectroscopy using the pyranine assay (as developed by Kamp, F., and Hamilton, J. A. (1992) *Proc. Natl. Acad. Sci. U.S.A. 89*, 11367−11370) shows that the transverse or flip-flop motion of long-chain FA (from 14 to 22 C atoms) is immeasurably fast in both small and large unilamellar EPC vesicles and characterized by half-times $t_{1/2} < 5$ ms. The rate-limiting step of FA transfer from these different donor systems to pyranine-containing EPC vesicles is the dissociation or desorption of the FA molecule from the donor. The desorption of the FA molecule is chain-length-dependent, confirming published data (Zhang et al. (1996) *Biochemistry 35*, 16055−16060): the first-order rate constant k_1 decreases by a factor of about 10 with elongation of the FA chain by two CH_2 groups. Similar rates of desorption are observed for the transfer of oleic acid from the three donors to pyranine-containing EPC vesicles with rate constants k_1 ranging from 0.4 to 1.3 s^{-1}. We also show that osmotically stressed, pyranine-containing EPC vesicles can give rise to artifacts. In the presence of a chemical potential gradient across the lipid bilayer of these vesicles, fast kinetic processes are observed with stopped-flow fluorescence spectroscopy which are probably due to electrostatic and/or osmotic effects.

Considerable research effort has been directed toward elucidating the mechanism of long-chain fatty acid (FA[1]) transport across cell membranes, and a knowledge of this mechanism is essential for an understanding of FA metabolism. Measurements using complex biological membranes have led to conflicting results and interpretations (*1*−*5*), and consequently FA transport across simple lipid bilayers has been studied. It has been argued that understanding the kinetics and thermodynamics of the steps of FA translocation in simple model systems will help in interpreting kinetic and thermodynamic data obtained with biological membranes. A number of studies have used model systems such as unilamellar lipid vesicles of different sizes and compositions to derive kinetic and thermodynamic information on FA translocation (*6*−*16*).

The three steps of FA translocation from the outer aqueous compartment across the lipid bilayer into the inner aqueous compartment of lipid vesicles can be represented by the following scheme:

$$FA_{water} \underset{k_{off}}{\overset{k_{on}}{\rightleftharpoons}} FA_{out} \underset{k_{ff}}{\overset{k_{ff}}{\rightleftharpoons}} FA_{in} \underset{k_{on}}{\overset{k_{off}}{\rightleftharpoons}} FA_{water} \qquad (1)$$

where FA_{water} is, as yet, undefined and represents FA present in water, FA_{out} and FA_{in} are FA molecules present in the outer and inner leaflets of the bilayer, respectively, k_{on} and k_{off} are the rate constants for FA association with the lipid bilayer and FA dissociation from the bilayer, respectively, and k_{ff} is the rate constant for FA transmembrane movement or flip-flop.

Since the solubility in water of native (physiological) FA with more than 14 C atoms is very low, FAs have to be administered in association with appropriate carriers or donors. Possible donors are protein−FA complexes, e.g., FA

† This work was supported by the Swiss National Science Foundation (Grant Nos. 32-46810.96 and 31-49726.96/1) and the Kamillo Eisner-Stiftung, CH-6062 Hergiswil, Switzerland.

* To whom correspondence should be addressed. E-mail: helmut.hauser@bc.biol.ethz.ch.

‡ Swiss Federal Institute of Technology.

§ University of Zürich.

|| University Hospital.

[1] Abbreviations: ADIFAB, rat intestinal fatty acid binding protein; BSA, bovine serum albumin; cmc, critical micellar concentration; EPC, egg phosphatidylcholine; FA, fatty acid molecule(s) without specification of the state of ionization; FA^-, deprotonated, ionized form of FA molecule(s); FAH, protonated, un-ionized form of FA molecule(s); LUV, large unilamellar vesicle; PC, phosphatidylcholine; POPC, 1-palmitoyl-2-oleoyl-*sn*-phosphatidylcholine; SUV, small unilamellar vesicle; TLC, thin-layer chromatography.

10.1021/bi011555p CCC: $22.00
Published on Web 01/11/2002

complexed with bovine serum albumin (BSA), and small unilamellar lipid vesicles (SUVs) containing FA in their lipid bilayer. The above scheme can be extended:

$$FA_{donor} \underset{k'_{on}}{\overset{k'_{off}}{\rightleftharpoons}} FA_{water} \underset{k_{off}}{\overset{k_{on}}{\rightleftharpoons}} FA_{out} \underset{k_{ff}}{\overset{k_{ff}}{\rightleftharpoons}} FA_{in} \underset{k_{on}}{\overset{k_{off}}{\rightleftharpoons}} FA_{water} \quad (2)$$

A key question that has been addressed in studies using simple lipid bilayers is the rate-limiting step. There is a general consensus that the rate of FA binding to lipid bilayers (characterized by the rate constant k_{on}) is extremely fast. This is consistent with a high value for the partition coefficient K describing the FA distribution between SUVs and water. This constant is to a first approximation given by $K = k_{on}/k_{off}$, and with the value of K reported for palmitate, 5×10^6 (*15*), and with $k_{off} = 5.6\ s^{-1}$, this yields a value for k_{on} of $2.8 \times 10^7\ s^{-1}$ (*11*). The question of the rate-limiting step is therefore reduced to determining whether the transverse (flip-flop) motion of FA or alternatively the FA dissociation from the donor particle (see eqs 1 and 2) is rate-limiting. Conflicting results have been reported in studies addressing this issue which cannot be explained in terms of differences in the model systems and methodology used. For instance, Hamilton and co-workers using SUVs and large unilamellar vesicles (LUVs) made mainly of egg phosphatidylcholine (EPC), FAs of different chain lengths, and various labeled FAs together with fluorescence spectroscopy showed that flip-flop is very fast, independent of the FA chain length, and that the dissociation of FA from the donor particle (eq 2) is rate-limiting (*8*, *10*−*12*). In contrast, Kleinfeld and co-workers using similar vesicles and methods interpreted kinetic data to indicate that flip-flop is rate-limiting (*6*, *9*, *13*, *14*). These authors also showed that the flip-flop rate depends on the FA chain length and the size and composition of the lipid vesicles (*13*, *14*). They inferred that FA transport across cell membranes is not suffuciently fast to match FA metabolic rates and proposed that FA transport is protein-mediated.

In an attempt to resolve some of this controversy in the literature, we repeated the measurements using essentially the same simple model systems as in the previous studies (*6*−*14*, *16*). The transfer of long-chain FA from various donor particles to both small and large unilamellar vesicles containing pyranine in the vesicle cavity was measured. It is our intention to extend these measurements to vesicles derived from the intestinal brush border membrane and to other FAs and bile salts.

EXPERIMENTAL PROCEDURES

Materials. EPC was purchased from Lipid Products (Nutfield, Surrey, U.K.), pyranine (8-hydroxy-1,3,6-pyrenetrisulfonate, trisodium salt), laser grade, was purchased from Arcos Organics (New Jersey), and myristic acid, stearic acid, oleic acid, eicosanoic acid, docosanoic acid, tetracosanoic acid, hexacosanoic acid, and FA-free BSA were purchased from Sigma. [9,10-^{3}H(N)]Oleic acid was from NEN Life Science Products (Geneva, Switzerland) and 1-palmitoyl-2-[1-^{14}C]oleoyl-*sn*-phosphatidylcholine from Amersham Switzerland.

Methods. (1) *Standard Buffer System*. The buffer used throughout was HEPES (*N*-(2-hydroxyethyl)piperazine-*N*′-2-ethanesulfonic acid, as the potassium salt) at a concentration of 10^{-1} M and pH 7.40, unless otherwise stated.

(2) Pyranine-Containing Lipid Vesicles. Aliquots of EPC in chloroform/methanol (2:1, v/v) were dried as a thin film, first by a stream of nitrogen and then under high vacuum for at least 1 h. The film was suspended, with vortexing, in aliquots of HEPES buffer containing 0.5 mM pyranine, to a final EPC concentration of ∼20 mg cm^{-3} (26.7 mM). Vesicles were produced by sonication using a Branson Sonifier 250 equipped with a microtip, operating a 100% duty cycle at a power setting of 1−1.5. During this process the sample was flushed with nitrogen and cooled in an ice bath. The samples were centrifuged (15000 rpm, 5 min) to remove metal fragments originating from the sonicator tip. Vesicles were freed of external pyranine by gel filtration on a Sepharose CL-4B column (30 × 1 cm) that had been equilibrated with HEPES buffer at room temperature, and were stored at 4 °C under nitrogen or argon.

Mixed EPC−oleate vesicles were prepared by the same method except that oleate (2 mol % relative to EPC) was included in the pyranine solution. Alternatively, small, known amounts of [^{3}H]oleic acid and [^{14}C]POPC were added to the EPC solution prior to drying, to facilitate quantitation. Concentration contributions of the radiolabels were ignored. Mixed EPC−very-long-chain FA (with 20 and more C atoms) vesicles were made by mixing the lipids in organic solvent and proceeding as described above.

LUVs were prepared by extrusion using a Lipex Biomembranes extruder and standard polycarbonate filters (Nucleopore). Lipid films were prepared as above, with the exception that the pyranine solution (0.5 mM) was made in 25 mM HEPES buffer. Samples were extruded five times through a 200 nm filter followed by five passes through a 100 nm filter under nitrogen pressure. Removal of external pyranine was as described for SUVs.

The average vesicle size, estimated from measurements on electron micrographs taken after freeze-fracture, was ∼25 nm for SUVs and ∼100 nm for LUVs. The purity of EPC was controlled before and after the FA transport measurement, and no chemical degradation was detected by TLC. Phospholipid concentrations were determined by total phosphate estimation (*17*).

(3) Sodium Oleate Dispersions. The appropriate amount of sodium oleate was added to HEPES buffer at room temperature and dispersed by brief sonication.

(4) BSA−Oleate Complexes. Stock solutions of BSA and oleate dispersions (as the sodium salt) were prepared in 0.1 M HEPES buffer. The BSA solution was dialyzed against the buffer overnight and the protein concentration determined using E (1%, 1 cm) = 6.67. BSA and oleate were mixed in suitable proportions, diluted appropriately, to prepare the 1:6 and 1:4 (mole ratio) BSA−oleate complexes, and incubated overnight at room temperature. The highest concentration of BSA used was 30 μM, and the ratios of oleate and BSA in the complexes were expressed as molar ratios.

(5) On-Line Fluorescence Measurements. Fluorescence measurements were carried out with a Fluorolog-2 double-monochromator spectrofluorimeter (Spex Industries, Inc., New Jersey) equipped with a thermostated cell holder and magnetic stirrer. All experiments were made with an excitation wavelength of 455 nm and emission wavelength of 512 nm, with slit widths that were as narrow as possible within

the constraint of maintaining good signal/noise ratios. Measurements were carried out at 20 °C. The time resolution was about 5 s determined by the manual mixing in the cuvette and the response time of the fluorimeter.

The external pH (pH_{out}) was measured in the fluorescence cell, using a suitably calibrated microelectrode (Mettler Toledo stomach probe, MIC, Solothurn, Switzerland), and the internal pH (pH_{in}) was monitored by the pyranine fluorescence. A calibration curve relating fluorescence intensity to pH_{in} was obtained as described previously (*8*). If required, lipid vesicles were permeabilized for protons by the addition of nigericin (1 μg/mg EPC) (*8*, *10*).

(6) Stopped-Flow Fluorescence Spectroscopy. Stopped-flow measurements were made with a Spectra Physics instrument with an estimated dead time of 5 ms and an SF-61 stopped-flow fluorimeter (High-Tech, Salisbury, England) with a dead time of 1 ms. In both instruments the sample syringes were maintained at 20 °C by means of a circulating water bath. In all experiments a 1:1 mixing ratio was used, and typically, 60 μL each of sample and reagent were mixed. Excitation was at 455 nm and fluorescence emission monitored using a 495 nm cutoff filter. Appropriate time bases for the sampling of the kinetic transients were determined in preliminary experiments, and a logarithmic time base was used in measurements on the SF-61 instrument. At least five scans were collected and averaged for each experiment. Averaged kinetic curves were fitted by single (eq 3), double, or higher order exponentials (eq 4).

$$y = y_\infty + Ae^{-kt} \tag{3}$$

$$y = y_\infty + \sum A_i e^{-k_i t} \tag{4}$$

y_∞ is the fluorescence signal intensity at equilibrium, A_i the amplitude of phase i, and k_i the corresponding apparent pseudo-first-order rate constant. Half-times $t_{1/2}$ were calculated from k_i as

$$t_{1/2} = (\ln 2)/k_i \tag{5}$$

The results of the curve-fitting procedures were confirmed by computer simulation using synthetic data based on experimentally determined parameters. For curve-fitting and kinetic calculations the Origin 4.1 software (from Microcal, Inc.) was used.

RESULTS

Pyranine-Containing SUVs Are Susceptible to Ionic Strength Gradients. To assess the suitability of the pyranine−EPC vesicle system as a model for the investigation of FA transport using stopped-flow fluorescence spectroscopy, established methods (*11*) were taken as a starting point. In this kind of experiment oleic acid, in a variety of forms, was mixed with unilamellar EPC vesicles containing pyranine. Internalization of the oleic acid results in the release of H^+ into the cavity of the vesicle, leading to the protonation of the dye, which causes a decrease in fluorescence intensity (*18*, *19*). A typical calibration curve, showing the response of pyranine-containing SUVs to pH changes, is shown in Figure 1. The apparent p*K* of entrapped pyranine derived

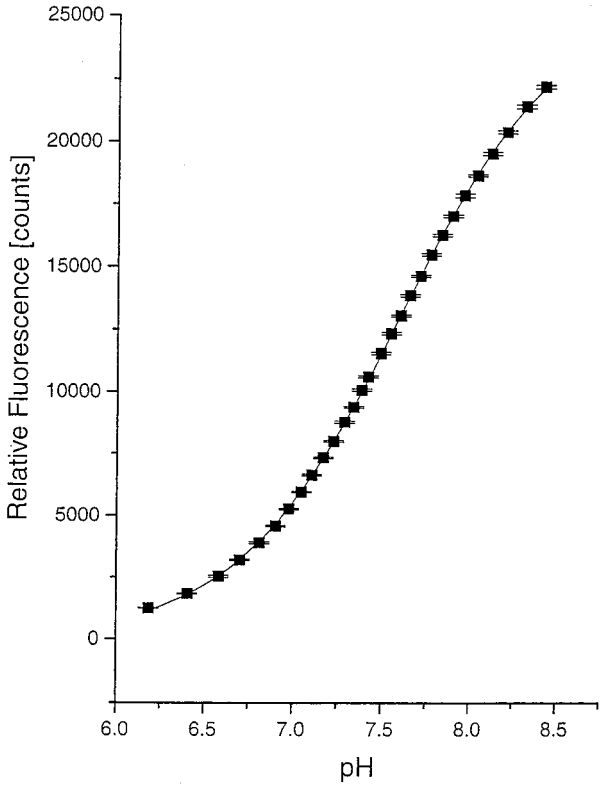

FIGURE 1: Fluorescence-monitored titration of pyranine-containing SUVs (300 μM in 0.1 M HEPES buffer, pH 7.6) with 2 M KOH, in the presence of nigericin (1 μg/mg EPC) at 20 °C. Nigericin was added to make the SUVs permeable to protons. The solid line is a fit to the experimental data using the Henderson−Hasselbach equation. In the Spex spectrofluorimeter an increase in fluorescence intensity corresponds to an apparent increase in pH.

by curve fitting was estimated to be 7.55 ± 0.01, higher than the p*K* of 7.22 reported for pyranine in aqueous solution (*18*).

In an initial series of experiments, aliquots of pyranine-containing EPC SUVs (260 μM) in HEPES buffer were mixed with equal volumes of dispersions of potassium oleate (12.5 μM, ~5 mol % relative to the EPC concentration) in 10^{-3} M KOH in the SF-61 stopped-flow apparatus. The kinetic curves obtained (Figure 2) were fitted by a biexponential function (eq 4), yielding two apparent pseudo-first-order rate constants, $k_1 = 53 \pm 2$ s^{-1} ($t_{1/2} = 13$ ms) and $k_2 = 1.3 \pm 0.1$ s^{-1} ($t_{1/2} = 0.53$ s) (Table 1). Control experiments, in which pyranine-containing SUVs were mixed with KOH alone, gave rise to an increase in fluorescence intensity corresponding to an acidification of the vesicle cavity. The kinetic trace thus obtained was fitted by a single exponential, yielding a pseudo-first-order rate constant k_1 of 21 ± 2 s^{-1} ($t_{1/2} = 33$ ms) (Table 2). The amplitude of the fluorescence intensity increase was about one-third of the change observed in experiments in which ~5 mol % oleate in 10^{-3} M KOH was mixed with EPC SUVs. Further experimentation in which simply water was mixed with SUVs showed that this induced a similar increase in fluorescence intensity.

The suspicion that these events were caused by changes in ionic strength initiated on mixing, and that they were probably due to electrostatic and/or osmotic effects, led to the experiments shown in Figure 3. Various KCl solutions were mixed with the vesicles up to a KCl concentration that

Table 1: Pseudo-First-Order Rate Constants k_1 and k_2 and Half-Times $t_{1/2}$ Obtained by Stopped-Flow Fluorescence Spectroscopy[a]

FA donor	type of vesicle	k_1 (s^{-1})	$t_{1/2}$ (s)	A (%)	k_2 (s^{-1})	$t_{1/2}$ (s)	A (%)
oleate in 10^{-3} M KOH	SUV	53 ± 2	0.013	56	1.3 ± 0.1	0.53	44
oleate in 10^{-3} M KOH	LUV	51 ± 3	0.014	54	1.6 ± 0.1	0.43	46
oleate dispersion in HEPES buffer	SUV	20 ± 5	0.035	53−66	0.40 ± 0.05	1.7	34−47
oleate dispersion in HEPES buffer	LUV	20 ± 4	0.035		0.45 ± 0.01	1.5	
BSA−oleate complex (1:6)	SUV	19 ± 5	0.037	78	0.7 ± 0.2	1	22
pH jump using mixed EPC−oleate vesicles	SUV	>140	<5 ms				
pH jump using mixed EPC−oleate vesicles	LUV	>140	<5 ms				

[a] Oleate was administered as a FA donor as defined in the first column. All vesicles (SUVs and LUVs) contained 0.5 mM pyranine in their cavities. Pseudo-first-order rate constants k_1 and k_2, half-times $t_{1/2}$, and amplitudes A expressed as percents were derived from curve fitting using eqs 3−5.

Table 2: Pseudo-First-Order Rate Constants k_1 and Half-Times $t_{1/2}$ Determined in Control Experiments Using Stopped-Flow and On-Line Fluorescence Spectroscopy[a]

no.	addition	type of vesicle	method	k_1 (s^{-1})	$t_{1/2}$ (s)
1	10^{-3} M KOH	pyranine-containing SUV	stopped-flow	21 ± 2	0.033
2	KCl of different concentrations (Figure 3)	pyranine-containing SUV	stopped-flow	21 ± 3	0.033
3	H^+ or OH^- to produce a proton gradient	pyranine-containing SUV	manual mixing	∼0.002	∼350
4	oleate dispersion in HEPES buffer	pyranine-containing SUV	manual mixing	∼0.0002	∼3500

[a] In experiments 3 and 4, proton leakage was measured. In experiment 3, a proton gradient was set up across the bilayer of pyranine-loaded vesicles and its slow dissipation was measured. In experiment 4, sodium oleate dispersed in HEPES buffer was added to pyranine-containing SUVs and proton leakage was measured after FA transport into pyranine-containing SUVs had reached equilibrium. Under these conditions the dissipation of the proton gradient balanced by the FA gradient was measured (cf. Figure 8).

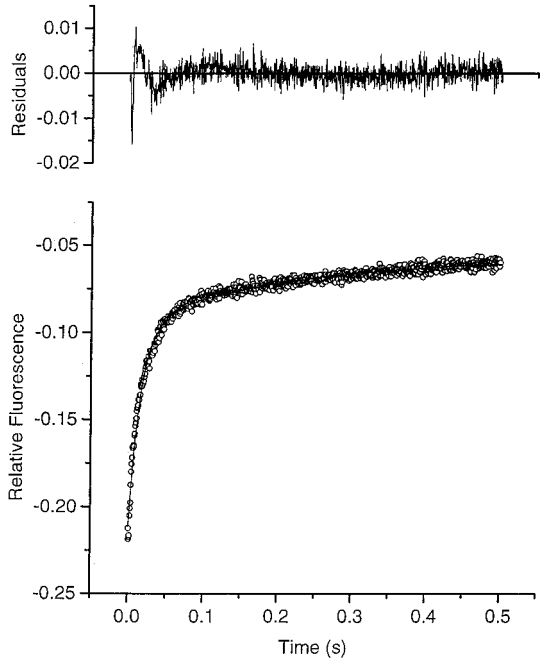

FIGURE 2: Kinetics of fluorescence intensity changes induced by stopped-flow mixing of a dispersion of 12.5 μM sodium oleate in 1 mM KOH with pyranine-containing EPC SUVs, 280 μM, dispersed in 0.1 M HEPES, pH 7.4. The upper panel shows the residuals of a double-exponential fit to a truncated fluorescence intensity curve. In stopped-flow experiments an increase in fluorescence intensity corresponds to a decrease in pH. A double-exponential fit was satisfactory for data points collected after 5 ms. The complete set of data points was adequately fitted by the sum of three exponentials, with the initial fast kinetic phase being within or faster than the time resolution of the instrument.

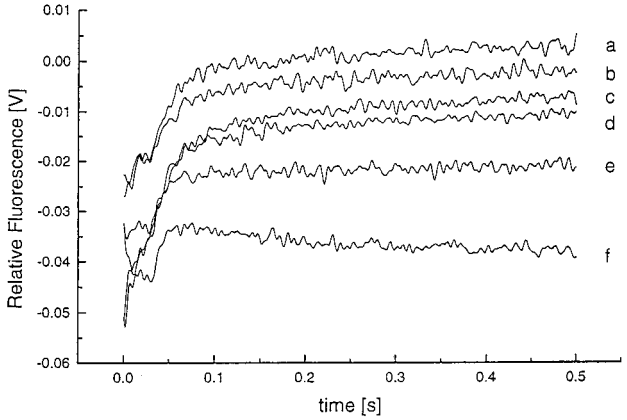

FIGURE 3: Kinetics of fluorescence intensity changes induced by adding increasing concentrations of aqueous KCl to pyranine-containing EPC SUVs. Stopped-flow mixing experiments in which SUVs, 300 μM in 0.1 M HEPES buffer, pH 7.4, were mixed with (a) 0, (b) 0.02, (c) 0.04, (d) 0.06, (e) 0.08, and (f) 0.1 M KCl produced solutions that contained 0.05 M HEPES and 0−0.05 M KCl.

produced a final ionic strength isosmolar with 0.1 M HEPES, the buffer concentration present in the interior of the vesicle. An increase in the fluorescence intensity was induced with an amplitude that was linearly related to the difference between the internal and external ionic strengths (data not shown). The time course of this process could be approximated by a single exponential from which an apparent pseudo-first-order rate constant k_1 of 21 ± 3 s^{-1} ($t_{1/2} = 33$ ms) was derived (Table 2).

Sodium Oleate Dispersions as a Donor System. These results indicate that it is important to maintain the ionic strength on mixing. Therefore, a variant on the basic experiment was performed, in which sodium oleate was simply dispersed in HEPES buffer. Such experiments have the advantage that there is no difference between the external and internal solvents under these conditions. Typical traces obtained when either SUVs or LUVs were mixed with oleate dispersions are shown in Figure 4. The data obtained with SUVs were well fitted by a double exponential, any deviation from the fit occurring at times close to the dead time of the stopped-flow device. The average values of the apparent rate

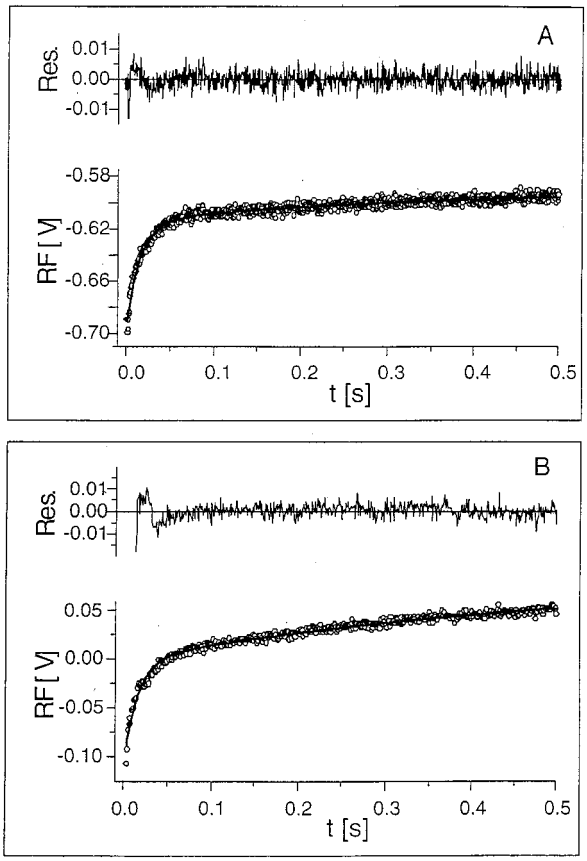

FIGURE 4: Kinetics of fluorescence intensity changes. (A) Stopped-flow mixing of a dispersion of sodium oleate, 7.5 μM in 0.1 M HEPES, pH 7.4, with pyranine-containing EPC SUV, 260 μM in 0.1 M HEPES, pH 7.4. The upper panel shows the residuals of a double-exponential fit to the data, the parameters of which are given in the text. RF expressed in volts is the relative fluorescence intensity. (B) Stopped-flow mixing of a dispersion of sodium oleate, 50 μM in 0.025 M HEPES, pH 7.4, with pyranine-containing EPC LUVs, 246 μM in 0.025 M HEPES, pH 7.4. The upper panel shows the residuals of a double-exponential fit to the data.

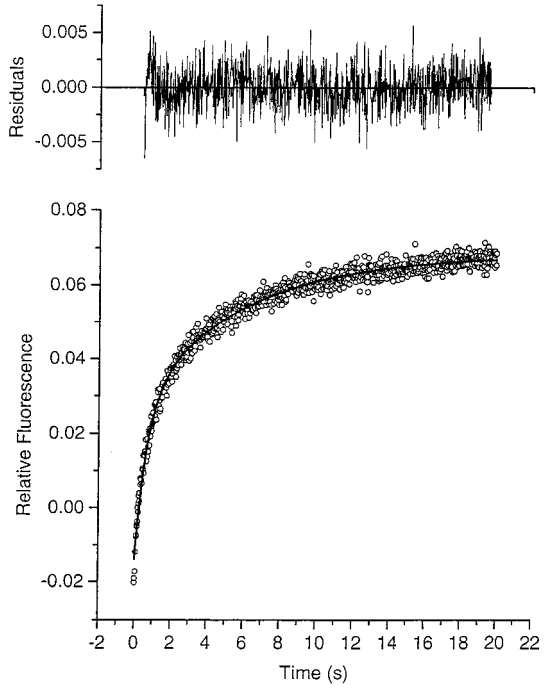

FIGURE 5: Kinetics of fluorescence intensity changes induced by stopped-flow mixing of a 1:6 (mole ratio) BSA−oleate complex in 0.1 M HEPES buffer, pH 7.4, with pyranine-containing EPC SUVs, 350 μM in 0.1 M HEPES buffer, pH 7.4. The total oleate concentration was 30 μM. The upper panel shows the residuals of a double-exponential fit to the data.

constants k_1 and k_2 derived from these data were 20 ± 5 s^{-1} ($t_{1/2} = 35$ ms) and 0.40 ± 0.05 s^{-1} ($t_{1/2} = 1.7$ s), respectively (Table 1). Both k_1 and k_2 were independent of both the oleate concentration (2.5−12 μM), keeping the SUV concentration constant at 260 μM, and the vesicle concentration (50−1.5 mM), with a constant oleate concentration of 12.5 μM. Similar results were obtained with LUVs (Figure 4B).

To measure proton leakage, manual mixing experiments with a longer time base were performed. After the initial, almost instantaneous acidification of the SUV cavity, there was a slow single kinetic phase, characterized by $k_1 \approx 0.0002$ s^{-1} ($t_{1/2} = 3500$ s), that restored the fluorescence signal to its original level (see Table 2).

BSA−Oleate Complexes as a Donor System. Serum albumin binds long-chain FA, suggesting that there are six sites for these ligands per albumin molecule and that 2−3 of the sites are of higher binding affinity (*20*−*22*). Dissociation constants for the complexes are quoted to be in the 10^{-6} to 10^{-8} M range (*23*, *24*). As a result, most of the oleic acid should be tightly bound in a 1:4 BSA−oleate complex, with a relatively low free FA concentration in solution, whereas the solution concentration should be higher in the 1:6 complex. In this donor system the BSA effectively buffers the free FA concentration. To test the properties of the BSA−oleate complex as a vehicle for the delivery of oleic acid to pyranine-containing SUVs, complexes were formed between FA-free BSA and oleic acid at these two molar ratios. As monitored by the acidification of the vesicle cavity, oleic acid was transferred from the 1:6 BSA−oleate complex to pyranine-containing SUVs in a process that could again be modeled by a double-exponential fit (Figure 5). Average values of the two apparent rate constants k_1 and k_2 were 19 $\pm$ 5 s^{-1} ($t_{1/2} = 37$ ms) and 0.7 $\pm$ 0.2 s^{-1} ($t_{1/2} = 1$ s), respectively (Table 1). Both k values were independent of the oleate concentration (6−30 μM), keeping the vesicle concentration constant at 360 μM, and also independent of the SUV concentration (0.1−1 mM), keeping the concentration of the BSA−oleate complex constant at [BSA] = 2.5 μM and [oleate] = 15 μM. Experiments with the 1:4 complex were unproductive under these experimental conditions, presumably reflecting the relative affinities of the SUVs and the BSA for oleate and the low free solution concentration of the FA.

As a necessary control to the experiments described above, FA-free BSA without oleate was mixed with the vesicle preparation, the concentration range of BSA chosen to mirror that used in the BSA−oleate complex experiments. The addition of BSA alone caused an apparent rise in internal pH possibly due to the removal of endogenous FA from the vesicles. It was estimated (*8*, *10*, *16*) that standard SUV preparations contain <0.2 mol % endogenous FA, the origin of which is presumably the result of either the partial hydrolysis of phosphatidylcholine during preparation or a contamination of the EPC stock.

Small Unilamellar Vesicles Containing 2 mol % FA as a Donor System. The kinetics of FA transfer between two populations of SUVs were determined using EPC SUVs (150

Table 3: Pseudo-First-Order Rate Constants k_1 and Half-Times $t_{1/2}$ for the Transfer of FA between Two Populations of EPC SUVs[a]

FA	k_1 (s^{-1})	$t_{1/2}$ (s)
myristic acid (C14:0)	20 ± 1	0.035
stearic acid (C 18:0)	0.213 ± 0.007	3.25
oleic acid (C18:1)	0.60 ± 0.01	1.2
eicosanoic acid (C20:0)	0.0224 ± 0.002	30.9
tetracosanoic acid (C24:0)	$0.000204 \pm 3 \times 10^{-5}$	3397.8

[a] Stopped-flow fluorescence spectroscopy was used for C14:0, C18:0, and C18:1, on-line fluorescence for C20:0 and C24:0. The experimental data were fitted adequately by a single-exponential decay, and the pseudo-first-order rate constants k_1 (s^{-1}) and half-times $t_{1/2}$ (s) were derived from curve fitting.

μM) with 2 mol % FA as the donor and pyranine-loaded EPC SUVs (150 μM) as the acceptor. The kinetic curves obtained were adequately fitted by a single-exponential function from which pseudo-first-order rate constants k_1 and half-times $t_{1/2}$ were derived (Table 3). These rate constants depended on the chain length of the FA and decreased by a factor of 10 with elongation of the FA chain by two CH_2 groups (Table 3). It was not possible to measure the transfer of hexacosanoic acid because proton leakage was faster than the transfer of this FA. These results are consistent with a previous report (*12*).

Transbilayer Transport of Oleic Acid Can Be Observed in Mixed EPC−Oleate Vesicles. An alternative method for the measurement of flip-flop rates is to induce FA translocation by means of an instantaneous "jump" in the external pH. This can be done, in a stopped-flow apparatus, by mixing EPC−FA vesicles dispersed in buffer at one pH with the same buffer at a slightly different pH. The sign of the initial pH gradient formed after the pH jump dictates the direction of transfer of the FA. A similar approach was used to investigate the flip-flop of 12-(9-anthroyloxy)stearic acid and very-long-chain FA in phospholipid bilayers (*11*, *12*). Mixed EPC−oleate SUVs, containing 2 mol % oleate, were prepared in 0.1 M HEPES buffer at pH 6.40, 7.47, and 8.40. Radiolabeled oleate and POPC were included so that the subsequent purification by gel filtration could be monitored by scintillation counting. The bulk of the oleate and EPC coeluted at the elution position of the vesicles at all three pH values, implying preferential incorporation of the FA in the EPC bilayer (data not shown). The pH jumps were designed to remain within the buffering range of HEPES and to have a magnitude on the order of that observed following the delivery of oleate to the vesicles (~0.5 pH unit). Aliquots of EPC−oleate SUVs at a particular pH were mixed, in turn, with buffers of different pH values. The resultant pH was determined in parallel experiments. Experiments in which EPC−oleate SUVs prepared at pH 7.47 were used are shown in Figure 6. The data measured after the SUVs were mixed with buffer at pH 7.47 were taken as a baseline value; i.e., there was no change in fluorescence under these conditions (Figure 6B). After the SUVs were mixed with buffer at either pH 6.4 or pH 8.4 (Figure 6A,C), there was an immeasurably rapid change in fluorescence that occurred within the mixing time of the stopped-flow device and was, therefore, characterized by a half-time of <5 ms (Table 1). Assuming that the only component of the system capable of transporting protons was the oleate, the rate of this process then represents that of the transverse (flip-flop) movement of oleic acid. The absolute amplitude of the fluorescence change was approximately equal for a given absolute change in pH, reflecting the approximately linear dependence of pyranine fluorescence on pH over the pH range studied (cf. Figure 1). The results were qualitatively the same for EPC−oleate SUV preparations at other pH values, the only difference being in the sign of the fluorescence change. Parallel experiments in which LUVs containing 10 mol % oleate were dispersed in 25 mM HEPES, pH 7.4, and then mixed with buffer at pH 8.4 (final pH 7.87) gave the same result (data not shown). When the pH jump was carried out with EPC SUVs containing myristic acid, stearic acid, or docosanoic acid each at 2 mol %, the same result was obtained as shown in Figure 6.

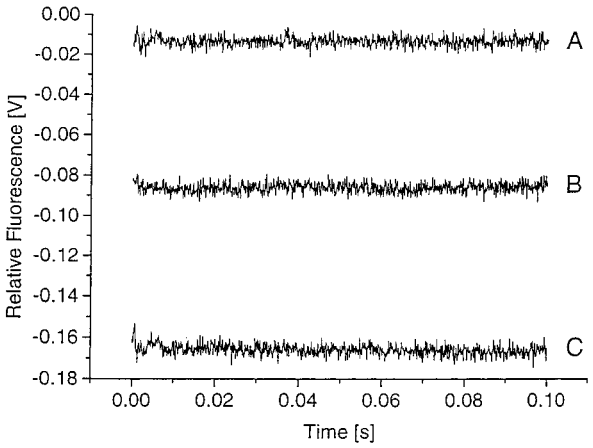

FIGURE 6: Measurements of stopped-flow fluorescence intensity changes induced by pH jump. Pyranine-containing EPC−oleate SUVs (2 mol % oleate), 265 μM, dispersed in 0.1 M HEPES buffer, initial pH 7.47, were mixed with 0.1 M HEPES buffer, pH 6.40, final pH 7.06 (A), with 0.1 M HEPES buffer, pH 7.47, final pH 7.47 (B), and with 0.1 M HEPES buffer, pH 8.40, final pH 7.87 (C).

To investigate further the effect of changes in external pH and the dissipation of pH gradients across the bilayer ("proton leakage"), EPC SUVs with pyranine entrapped in their cavity (without added oleate) were prepared at either pH 6.4 or pH 8.4, both were manually mixed, in separate experiments, with an equal volume of buffer at pH 6.4 or 8.4, and the progress of the resultant process was followed fluorimetrically. Data gathered following the addition of pH 8.40 buffer to SUVs prepared at pH 6.40 (final pH 7.47) are shown in Figure 7. This addition caused an event of a biphasic nature, the effective starting point of which was the signal intensity of SUVs diluted 1:1 with pH 6.40 buffer (Figure 7a). The first phase was too rapid to be resolved by this method (Figure 7b) and was followed by a much slower second phase that was characterized by an apparent pseudo-first-order rate constant k_1 of ~0.002 s^{-1} ($t_{1/2} = 350$ s) (Table 2). Figure 7c shows the signal intensity 1.45 h after the SUVs were mixed with buffer, while the end point of the process could be estimated following the addition of nigericin (Figure 7d). Quantitatively similar results were obtained when the pH jump was reversed. It should be noted that the rate of proton leakage was very slow in relation to the other kinetic events, and it has been assumed that this does not affect the analysis of the faster kinetic events.

DISCUSSION

Difficulties and Possible Errors in FA Transport Measurements. The complex phase behavior of FA introduces certain

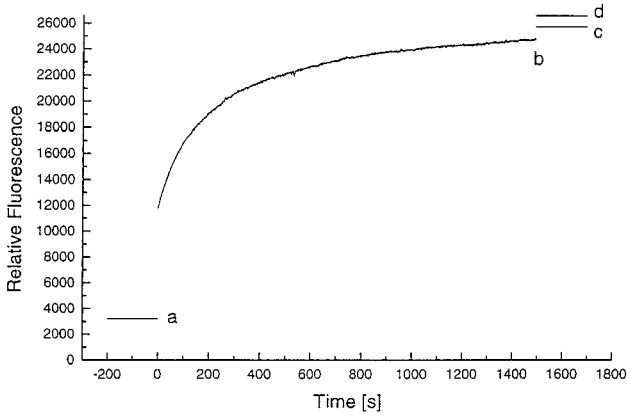

FIGURE 7: Kinetics of fluorescence intensity changes induced on mixing of EPC SUVs, 260 μM, dispersed in 0.1 M HEPES buffer, pH 6.4, with the same buffer at pH 6.4 (a) and pH 8.4 (b). The fluorescence signal intensity after 1.45 h is shown in (c) and the intensity following the addition of 5 μL nigericin (0.1 mg cm^{-3} in ethanol) in (d). These experiments were performed using the on-line Spex fluorimeter.

difficulties. Long-chain FAs are, like all lipids, poorly soluble in water and exhibit a high tendency to self-assemble in an aqueous medium, forming a variety of lipid aggregates (phases). The nature of the lipid phase formed depends on the type of lipid, the lipid concentration, and experimental conditions such as temperature, pH, ionic strength, and ionic composition. At neutral pH, the solubility in water or cmc of oleic acid/oleate is <1 μM (*25*), and at concentrations $>$cmc this compound forms a lamellar phase (*26*, *27*); i.e., in excess water unilamellar FA vesicles are present (*28*, *29*). In contrast, in the fully ionized state at pH $\geq$ 11 sodium oleate forms micelles (*27*).

The determination of the cmc of oleate is difficult and subject to large errors. Published values for the cmc at neutral pH vary widely, ranging from submicromolar concentrations to 6 μM (*25*, *30*). Most measurements reported here were carried out at FA concentrations >6 μM, i.e., at concentrations above the cmc. The experimental conditions used here are such that the concentration of monomeric FA is relatively low compared to the total FA concentration.

The results presented clearly show that the experimental rate constants measured for FA transport, at least those of the initial fast kinetic phase, depend on the way in which the FA is delivered to unilamellar vesicles, and artifacts may be produced in this way. Difficulties arising when ethanolic solutions of FA are added to pyranine-containing SUVs were discussed previously (*13*). In many of the previous studies FAs were delivered as a salt in alkaline solution or in dilute nominal buffer at pH values far from the p*K* of the buffer. These solutions were mixed with vesicles dispersed in a relatively concentrated buffer at approximately neutral pH such that there was effectively no pH change in the vesicle dispersion. However, the equilibrium of the original FA phase was markedly perturbed, leading to time-dependent phase changes. Such phase changes will affect the FA transport measurement and complicate the interpretation of these measurements. Indeed, the kinetic curves obtained for oleate transport into SUVs (Figure 2) or LUVs are quite complex when the FA is added in 10^{-3} M KOH. Sometimes these curves could not be fitted by less than three exponential terms. With double-exponential fits as shown in Figure 2, the rapid kinetic phase was characterized by values of $k \geq 50$ s^{-1} ($t_{1/2} \leq 14$ ms) that were significantly higher than those obtained when oleate was administered as a dispersion in buffer or as a complex with BSA (Table 1). These *k* values may well reflect FA phase changes induced on mixing of the alkaline oleate dispersion with lipid vesicles rather than oleate transport.

Control experiments clearly indicate that the generation of a chemical potential gradient across the lipid bilayer gives rise to artifacts. Mixing of the vesicles with not only KOH but also H_2O and sub-isosmolar KCl solutions led to fluorescence changes that apparently correspond to an acidification of the internal cavity (Figure 3). Upon mixing of water or a 10^{-3} M KOH solution with SUVs dispersed in 0.1 M HEPES, pH 7.4, the ionic strength of the buffer is halved, resulting in a salt gradient across the vesicle bilayer. It is not clear by which mechanism the salt gradient affects the pyranine fluorescence in a way that corresponds to an acidification of the vesicle cavity, but the underlying cause is very likely to be electrostatic and/or osmotic in origin. Vesicles respond to osmotic stress by swelling or shrinking due to influx or efflux of water depending on the direction of the applied gradient (*31*−*33*). The apparent p*K* of pyranine is 7.55 when entrapped in SUVs. This is higher than the value of 7.22 measured for pyranine in aqueous solution (*18*, *19*), suggesting interaction of the dye with the internal vesicle surface. Swelling and shrinking of the vesicles alters the geometric properties of the internal surface, and this type of change might well affect the interaction of pyranine with the vesicle surface, thus altering the fluorescence intensity. Results obtained with the KCl mixing experiments (Figure 3) have not been reported previously. This artifact demonstrates how important it is to avoid changes in pH and ionic strength in the course of FA transport measurements. However, it should be stressed that this kind of artifact is only observed with stopped-flow fluorescence but not with on-line flourescence. Therefore, results previously obtained with the pyranine method and on-line fluorescence are not affected by this problem.

In measuring biphasic kinetics by stopped-flow fluorescence spectroscopy, the correct choice of the timebase is crucial (*34*−*37*) as substantial errors in the kinetic parameters can be introduced by the use of inappropriate timebases for data acquisition. A satisfactory solution to the problem is to employ a logarithmic timebase as the sampling intervals then mirror the exponential nature of the processes involved (*34*−*37*). In this work the primary fluorescence data were acquired with logarithmic timebases or timebases judged appropriate as a result of logarithmic timebase trial runs.

We have used the pH-sensitive fluorophore pyranine entrapped in the cavity of SUVs or LUVs to measure pH changes induced by the addition of FA, the same methodology as was used by different groups to measure the kinetics of FA desorption from lipid bilayers and FA flip-flop across lipid bilayers (*8*, *10*−*14*). This methodology has the advantage that native (physiological) FA can be used. Methods based on fluorescent-labeled FA are subject to criticism since the physicochemical properties of fluorescent-labeled FA can differ significantly from those of native FA, and the kinetic parameters derived from these measurements may not be representative (*6*, *9*−*11*, *14*).

Kinetics of Transverse (Flip-Flop) Movement of Long-Chain FA. EPC SUVs and EPC LUVs both containing 2 mol % FA dispersed in HEPES buffer are used in this experiment. We treat here the inner and outer leaflets of the vesicle bilayer as equivalent environments, which is true for sufficiently large vesicles and to a first approximation for SUVs. Since the p*K* of long-chain FA embedded in lipid bilayers is 7.6 (*7*), approximately equal concentrations of protonated and ionized FA are present in both the inner and outer leaflets of the bilayer at pH 7.4. It was shown before (*8*, *10*) that the protonated (uncharged) form of FA (FAH) is capable of undergoing flip-flop whereas the same movement of the deprotonated (ionized) FA molecule (FA^-) is very slow and characterized by rate constants of $<10^{-4}$ s^{-1} (*38*). The concentrations of FAH in the inner and outer leaflets of the bilayer are in equilibrium, i.e., $[FAH_{in}]/[FAH_{out}] = K_{ff}$, with the value of this equilibrium constant being presumably close to 1 and independent of the pH. If the external pH is decreased by a pH jump, there is an increase in FAH molecules present in the outer monolayer. Some of these molecules move across the bilayer to reestablish the equilibrium characterized by K_{ff}. In so doing, protons are transported across the bilayer, and some are subsequently released into the internal cavity, thus lowering the pH. At equilibrium the total FA (protonated plus deprotonated) concentration of the inner leaflet is greater than that in the outer leaflet (cf. Figure 8C). There is an outwardly oriented FA concentration gradient balanced by a proton gradient of opposite sign (Figure 8C). The opposite situation is found when the sign of the pH jump is reversed.

The interpretation of the pH-jump measurement is therefore straightforward: the instantaneous change in fluorescence intensity represents the redistribution of FAH molecules across the phospholipid bilayer, i.e., the transverse or flip-flop movement of FA in the direction dictated by the sign of the applied pH gradient (Figure 6) (*11*, *12*, *39*). In principle, the pH jump could produce an internal pH change by the simple transbilayer movement of protons accompanied, if necessary, by counterions. The manual pH jump experiments (Figure 7) rule out this possibility. The instantaneous change in fluorescence intensity (Figure 7) is probably due to FA-mediated proton translocation. The FA present in the phospholipid bilayer is very likely a contamination arising from the breakdown of PC molecules during sonication. The second slow phase observed in the manual pH jump can be attributed to proton leakage, a process characterized by a half-time of ~10 min (*8*, *10*) (Table 2) and enhanced in the presence of nigericin (Figure 7).

We can therefore conclude that the fast process characterized by a half-time of less than 5 ms (Figure 6) represents the transverse (flip-flop) motion of long-chain FA (FA with 14−22 C atoms). Therefore, this motion cannot be the rate-limiting step in FA transfer between lipid vesicles. These conclusions are in agreement with some of the published work. Hamilton and co-workers reported that the flip-flop of different FAs (14−18 C atoms) in SUVs (diameter ~25 nm) is immeasurably fast ($t_{1/2} < 5$ ms) and the equilibrium distribution of FA between the two leaflets of the bilayer is reached within the mixing or dead time of the instrument (*11*). However, for LUVs (diameter ~100 nm) the same authors reported fast but still measurable flip-flop for long-chain FA with a half-time $t_{1/2}$ of 23 ± 12 ms (*11*). We are

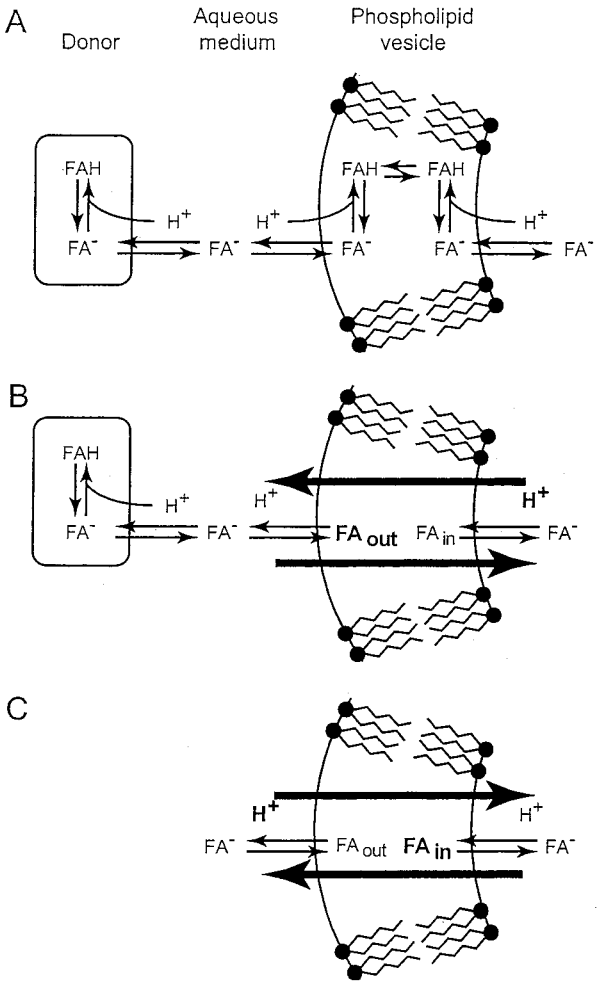

FIGURE 8: (A) Various equilibria involved in FA transport across a lipid bilayer. FA donors are either FA vesicles or phospholipid vesicles containing FA in their lipid bilayer or BSA−FA complexes. (B) Opposing gradients present at equilibrium after addition of FA as an FA donor to EPC SUVs. FA molecules present in the aqueous phase and in equilibrium with the FA donor are incorporated in the outer leaflet of the phospholipid vesicle bilayer. FAH molecules undergo flip-flop to the inner leaflet of the bilayer, releasing protons into the vesicle cavity. At equilibrium two opposing gradients exist across the vesicle bilayer (represented by large bold arrows), an inwardly directed FA gradient and an outwardly directed proton gradient. (C) Opposing gradients (represented by large bold arrows) set up by a pH jump. Decreasing the external pH by a pH jump causes FAH molecules to move to the inner leaflet of the bilayer. At equilibrium the inwardly directed proton gradient is balanced by an outwardly directed FA gradient.

unable to reproduce this result. In our hands the flip-flop rate of oleic acid was immeasurably fast and the process complete in <5 ms in both SUVs and LUVs. Therefore, we are unable to say whether the FA flip-flop rate depends on the vesicle size. Our results for the flip-flop of long-chain FA in phospholipid bilayers are inconsistent with data reported by Kleinfeld and co-workers. These authors concluded from stopped-flow fluorescence spectroscopy using the fluorescent probe ADIFAB (*14*) and differently sized vesicles (LUVs of diameter ~100 nm and giant unilamellar vesicles of diameter >200 nm) composed of EPC and cholesterol that flip-flop is the rate-limiting step in FA transport across lipid bilayers (*6*, *9*, *13*). Values obtained for the flip-flop rate constant of oleic acid across EPC/cholesterol bilayers (mole ratio 2:1 to 3:1) at 20 °C were

$k_{ff} = 3\ s^{-1}$ ($t_{1/2} = 230$ ms) for LUVs and $k_{ff} = 0.1\ s^{-1}$ ($t_{1/2} = 6.9$ s) for giant unilamellar vesicles. Kleinfeld and co-workers also reported that the rate constants for flip-flop of FA depend on the FA chain length.

Kinetics of FA Transport into SUVs and LUVs Using Different Donor Systems. When the FA is delivered externally to phospholipid vesicles, either as an oleate dispersion (Figure 4) or as a BSA−oleate complex (Figure 5), at time zero there is an initial equilibrium between free FA and the aggregated state of FA, and there is no FA present in the EPC vesicle. It has been shown that the rate of FA binding to the external bilayer surface and the subsequent incorporation of FA into the vesicle bilayer are very fast (*6*, *10*, *14*). In this way, a potential gradient of FA between the outer and inner leaflets is created (Figure 8B) and the system responds to the concentration imbalance by the internalization of FAH molecules. Upon arrival at the internal vesicle surface some of the FAH molecules dissociate according to the effective p*K*, releasing protons into the internal cavity and lowering the internal pH. This drop in pH, however, opposes the transfer of further FAH molecules, and at equilibrium, there is a balance across the bilayer between two opposing gradients: an outwardly oriented proton gradient and an inwardly oriented FA gradient. Thus, at equilibrium, the total concentrations of FAH and FA in the outer and inner leaflets are not the same and the internal and external proton concentrations are also different (Figure 8B).

In both types of experiments (Figures 4 and 5) the situation in which there is a balance between opposing concentration gradients will pertain unless the system is disturbed in some way. Proton leakage will lead not only to the dissipation of the pH gradient but also to the redistribution of FA within the bilayer. The apparent leakage rate measured after the addition of a FA dispersion ($t_{1/2} = 3500$ s) is markedly slower than that measured in the absence of a FA gradient ($t_{1/2} =$ 350 s) (cf. Table 2).

Biphasic kinetics are observed for FA transport into phospholipid vesicles when FA is supplied either as a dispersion (Figure 4) or as a BSA−FA complex (Figure 5). The slower phase, characterized by the rate constant k_2, is almost certainly due to the dissociation of FA from either FA aggregates or the BSA−oleate complex. Dissociation occurs in response to FA binding to phospholipid vesicles and lowering the free FA concentration in water, with which the FA aggregates or BSA−FA complex is initially in equilibrium. The supply of FA is then limited by the rate of hydration of the FA molecule as FA leaves the aggregate or complex (*40*). The value $k_2 = 0.40\ s^{-1}$ for the desorption of oleate from oleate bilayers (Table 1) is on the same order as the rate constant obtained for the desorption of oleate from phospholipid SUVs (Table 3) (*12*). The value of the rate constant $k_2 = 0.7\ s^{-1}$ ($t_{1/2} = 1$ s) (Table 1) is characteristic for the rate of oleate dissociation from BSA consistent with published data (*41*).

The assignment of the fast kinetic phases observed when oleate was added either as a dispersion or as a BSA complex is more difficult. The k_1 values characteristic of this phase are identical within the error of the measurement (Table 1). Since these values are also identical to the apparent pseudo-first-order rate constants (cf. Tabels 1 and 2) characteristic of the electrostatic−osmotic processes observed in the absence of FA, the fast kinetic phase (in Figures 4 and 5) is possibly due to an artifact. This kinetic phase cannot be assigned to the incorporation of FA in the outer leaflet of the bilayer; first, this interaction was shown to be very fast, characterized by rate constant $k_{on} = 2.8 \times 10^7\ s^{-1}$ (*11*), and second, it involves collisional interactions which are at least bimolecular, giving rise to second-order kinetics.

In contrast, our kinetic analysis of FA transfer from FA bilayers or BSA−FA complexes to phospholipid vesicles shows that the rate-limiting step is a true first-order process. The dissociation of FA from FA aggregates and FA−protein complexes and the transverse movement (flip-flop) of FA molecules are both unimolecular, giving rise to first-order kinetics. From our kinetic analysis we conclude that the rate-limiting step of FA transfer is the dissociation (desorption) characterized by k_{off} (eq 2). This conclusion is corroborated by the FA transfer measured between two populations of SUVs. Since the flip-flop of FA was shown to be very fast, the single-exponential process observed in these measurements was interpreted to reflect the desorption of FA from the EPC bilayer. As shown in the Appendix, the observed rate constant k_{obsd} derived from curve fitting is identical to the rate constant k_{off}. The k_{off} values (Table 3) derived from these measurements agree within 1 order of magnitude with rate constants published for the desorption of FA from lipid bilayers (*12*, *41*−*43*). The main conclusion of our kinetic analysis is that the desorption of FA is rate-limiting. This conclusion is in agreement with some published data (*8*, *10*−*12*, *40*−*44*), but at variance with others (*6*, *9*, *13*, *14*). The fact that the rate constant k_{off} is a true first-order rate constant indicates that FA transfer from various donor systems to the acceptor vesicles proceeds through the aqueous phase and not through collisional contacts (*6*, *9*, *40*, *43*, *44*).

Physiological Significance. FA plays a central role in lipid metabolism. The question of the mechanism of FA transport into and out of cells and across cell membranes has been the subject of extensive studies and discussions. Using cellular systems, these studies have led to conflicting conclusions: FA transport across cell membranes has been interpreted either as passive diffusion (*45*, *46*) or as a protein-mediated process (*1*, *3*, *47*−*54*). Our present in vitro study shows that the transverse or flip-flop movement of physiological FA is very fast with half-times $t_{1/2} < 5$ ms and that the desorption of FA from the aggregated state is rate-limiting (*8*, *10*−*12*, *40*, *43*, *44*). The justification of in vitro studies is the expectation that they will help to elucidate the mechanism of FA transport in vivo. It has been argued that the demonstration of rapid, unfacilitated movement of FA across lipid bilayers makes this a potentially viable mechanism in biological membranes (*8*, *10*−*12*). However, under physiological conditions, low concentrations of free FA may prevail and protein-mediated (facilitated) transport of FA across cell membranes may become important. We believe that in studying the mechanism of FA transport across biological membranes, particularly the question of passive versus facilitated FA transport, the adjustment of the free FA concentrations to levels prevailing under physiological conditions is crucial for obtaining relevant kinetic data. The key issue of whether FA transport across biological membranes is a passive or facilitated/active process remains a matter of debate. It should, however, be clear that this issue cannot be resolved by studies using models such as lipid

bilayers. Studies on real biological membranes under physiologically relevant conditions as well as in vivo (animal) experiments are required to provide an answer to this important question.

APPENDIX

Since the flip-flop movement of FA was shown to be immeasurably fast, eq 2 reduces to

$$FA_{donor} \underset{k'_{on}}{\overset{k'_{off}}{\rightleftharpoons}} FA_{water} \underset{k_{off}}{\overset{k_{on}}{\rightleftharpoons}} FA_{out} \quad (6)$$

Upon mixing of FA donor and pyranine-containing EPC vesicles, the following differential equations can be written:

$$\frac{d[FA_{donor}]}{dt} = k'_{on}[FA_{water}][D] - k'_{off}[FA_{donor}] \quad (7)$$

$$\frac{d[FA_{water}]}{dt} = k'_{off}[FA_{donor}] + k_{off}[FA_{vesicle}] - k'_{on}[FA_{water}][D] - k_{on}[FA_{water}][A] \quad (8)$$

where $[FA_{water}]$, $[FA_{donor}]$, and $[FA_{vesicle}]$ are the FA concentrations in water, in the donor, and in the vesicle, respectively. [D] is the donor concentration and [A] the concentration of EPC vesicles. With the reasonable assumption that $d[FA_{water}]/dt \rightarrow 0$, and that to a first approximation $k_{on} = k'_{on}$ and $k'_{off} = k_{off}$, the solution of the above differential equations is eq 9,

$$\frac{[FA_{donor}]}{[FA_{donor}]_0} = y_\infty + (1 - y_\infty)e^{-k_{off}t} \quad (9)$$

where $[FA_{donor}]_0$ is the total FA concentration present in the donor at time $t = 0$ and $y_\infty = [D]/([D] + [A])$. It follows from eq 9 that $[FA_{donor}]/[FA_{donor}]_0$ is 1 or 100% at $t = 0$ and this ratio (percentage) decreases exponentially from 1 (100%) to an equilibrium value y_∞. Equation 9 is apparently identical with eq 3, and hence $k_{obs} = k_{off}$. The observed rate constant, i.e., the rate constant derived from curve fitting, is identical to k_{off}, the rate constant defining the rate-limiting step.

REFERENCES

1. Storch, J. (1990) *Hepatology 12*, 1447−1449.
2. Kleinfeld, A. (1995) in *Stability and Permeability of Lipid Bilayers* (Disalvo, E. A., and Simon, S., Eds.) pp 241−258, CRC Press, Boca Raton, FL.
3. Abumrad, N., Harmon, C., and Ibrahimi, A. (1998) *J. Lipid Res. 39*, 2309−2318.
4. Hamilton, J. A. (1998) *J. Lipid Res. 39*, 467−481.
5. Schulthess, G., Werder, M., and Hauser, H. in *Fat Digestion and Absorption* (Christophe, A. B., and De Vriese, S., Eds.) pp 60−95, AOCS Press, Champaign, IL.
6. Storch, J., and Kleinfeld, A. M. (1986) *Biochemistry 25*, 1717−1726.
7. Hamilton, J. A., and Cistola, D. P. (1986) *Proc. Natl. Acad. Sci. U.S.A. 83*, 82−86.
8. Kamp, F., and Hamilton, J. A. (1992) *Proc. Natl. Acad. Sci. U.S.A. 89*, 11367−11370.
9. Kleinfeld, A. M., and Storch, J. (1993) *Biochemistry 32*, 2053−2061.
10. Kamp, F., and Hamilton, J. A. (1993) *Biochemistry 32*, 11074−11086.
11. Kamp, F., Zakim, D., Zhang, F., Noy, N., and Hamilton, J. A. (1995) *Biochemistry 34*, 11928−11937.
12. Zhang, F., Kamp, F., and Hamilton, J. A. (1996) *Biochemistry 35*, 16055−16060.
13. Kleinfeld, A. M., Chu, P., and Storch, J. (1997) *Biochemistry 36*, 5702−5711.
14. Kleinfeld, A. M., Chu, P., and Romero, C. (1997) *Biochemistry 36*, 14146−14158.
15. Noy, N., Donnelly, T. M., and Zakim, D. (1986) *Biochemistry 25*, 2013−2021.
16. Kleinfeld, A. M., Storms, S., and Watts, M. (1998) *Biochemistry 37*, 8011−8019.
17. Ames, B. N. (1966) *Methods Enzymol. 8*, 115−118.
18. Kano, K., and Fendler, J. H. (1978) *Biochim. Biophys. Acta 509*, 289−299.
19. Clement, N. R., and Gould, J. M. (1981) *Biochemistry 20*, 1534−1538.
20. Spector, A. A., John, K., and Fletcher, J. E. (1969) *J. Lipid Res. 10*, 56−67.
21. Hamilton, J. A., Era, S., Bhamidipati, S. P., and Reed R. G. (1991) *Proc. Natl. Acad. Sci. U.S.A. 88*, 2051−2054.
22. Carter, D. C., and Ho, J. X. (1994) *Adv. Protein Chem. 45*, 153−203.
23. Goodman, D. S. (1958) *J. Am. Chem. Soc. 80*, 3892−3898.
24. Spector, A. A., and Fletcher, J. E. (1978) in *Disturbances in Lipid and Lipoprotein Metabolism* (Dietschy, J. M., Gotto, A. M., and Ontko, J. A., Eds.) pp 229−248, American Physiological Society, Rockville, MD.
25. Vorum, H., Broderson, R., Kragh-Hansen, U., and Pedersen, A. O. (1992) *Biochim. Biophys. Acta 1126*, 135−142.
26. Small, D. M. (1986) *The Physical Chemistry of Lipids: from Alkanes to Phospholipids*, Handbook of Lipid Research Series, Vol. 4, pp 385−393, Plenum, New York.
27. Cistola, D. P., Hamilton, J. A., Jackson, D., and Small, D. M. (1988) *Biochemistry 27*, 1881−1888.
28. Gebicki, J. M., and Hicks, M. (1973) *Nature 243*, 232−234.
29. Gebicki, J. M., and Hicks, M. (1976) *Chem. Phys. Lipids 16*, 142−160.
30. Richieri, G. V., Ogata, R. T., and Kleinfeld, A. M. (1992) *J. Biol. Chem. 267*, 23495−23501.
31. Bittmann, R., and Blau, L. (1972) *Biochemistry 11*, 4831−4839.
32. De Gier, J. (1993) *Chem. Phys. Lipids 64*, 187−196.
33. Lerebours, B., Wehrli, E., and Hauser, H. (1993) *Biochim. Biophys. Acta 1152*, 49−60.
34. Walmsley, A. R., and Bagshaw, C. R. (1989) *Anal. Biochem. 176*, 313−318.
35. Crabbe, M. J. C. (1981) *Methods Biochem. Anal. 31*, 417−474.
36. Hiromi, K. (1979) *Kinetics of Fast Enzyme Reactions*, Wiley, NewYork.
37. Bernasconi, X. X. (1976) *Relaxation Kinetics*, Academic Press, New York.
38. Gutknecht, J. (1988) *J. Membr. Biol. 106*, 83−93.
39. Hope, M. J., and Cullis, P. R. (1987) *J. Biol. Chem. 202*, 4360−4366.
40. Doody, M. C., Pownall, H. J., Kao, Y. J., and Smith, L. C. (1980) *Biochemistry 19*, 108−116.
41. Massey, J. B., Bick, D. H., and Pownall, H. J. (1997) *Biophys. J. 72*, 1732−1743
42. Weisiger, R. A., and Ma, W. L. (1987) *J. Clin. Invest. 79*, 1070−1077.
43. Daniels, C., Noy, N., and Zakim, D. (1985) *Biochemistry 24*, 3286−3292.
44. Sengupta, P., Sackmann, E., Kuhnle, W., and Scholz, H. P. (1976) *Biochim. Biophys. Acta 436*, 869−878.
45. Bröring, K., Haest, C. W. M., and Deuticke, B. (1989) *Biochim. Biophys. Acta 986*, 321−331.
46. Cooper, R. B., Noy, N., and Zakim, D. (1989) *J. Lipid Res. 30*, 1719−1726.
47. Abumrad, N. A., Perkins, R. C., Park, J. H., and Park, C. R. (1981) *J. Biol. Chem. 256*, 9183−9191.
48. Abumrad, N. A., Park, J. H., and Park, C. R. (1984) *J. Biol. Chem. 259*, 8945−8953.

49. Spector, A. A. (1986) *Biochemistry and Biology of Plasma Lipoproteins*, Vol. 2, pp 247−279, Dekker, New York.
50. Paulussen, R. J. A., and Veerkamp, J. H. (1990) in *Subcellular Biochemistry* (Hilderson, H. J., Ed.) pp 175−181, Plenum Press, New York.
51. Stremmel, W., Strohmeyer, G., Borchard, F., Kochwa, S., and Berk, P. D. (1985) *Proc. Natl. Acad. Sci. U. S.A. 82*, 4−8.
52. Stremmel, W., Lotz, G., Strohmeyer, G., and Berk, P. D. (1985) *J. Clin. Invest. 75*, 1068−1076.
53. Stremmel, W., Strohmeyer, G., and Berk, P. D. (1986) *Proc. Natl. Acad. Sci. U.S.A. 83*, 3584−3588.
54. Stremmel, W. (1988) *J. Clin. Invest. 82*, 2001−2010.

BI011555P